Coverage Analysis of a THz Aerial Base Station Wireless Network in a Finite Area

Hadeel Obaid*, Yongxu Zhu†, Bo Tan*
*Faculty of Information Technology and Communication Sciences, Tampere University, Finland;
†National Communications Research Laboratory, Nanjing, China
{hadeel.obaid, bo.tan}@tuni.fi
yongxu.zhu@seu.edu.cn

***Abstract*—Terahertz (THz) transmission technologies show great promise in enabling ultra-broadband short-range in the next-generation communications. The incorporation of THz transmission with Aerial Base Stations (ABS) networks offers promising advantages, particularly in establishing favorable ultra-broadband line-of-sight links. In this paper, we provide a performance analysis for a finite THz ABS network serving a given region. We model the spatial distribution of the ABSs as a binomial point process within an overlapped finite circular area. To derive the coverage probability, we consider a probabilistic model that encompasses both line-of-sight and non-line-of-sight propagation scenarios, and a user association policy based on the strongest average received power. The association probabilities and Laplace transform of the interference are also derived. The derived coverage probability is validated through Monte Carlo simulation. We further investigate the impacts of the ABS's height and the radius of the area on the coverage performance.**

***Index Terms*—Aerial base station, Terahertz, Stochastic Geometry, binomial point process, coverage probability.**

I. Introduction

Research and applications involving wireless communication with Aerial base stations (ABS) are on the rise, driven by the mobility and cost-effectiveness they offer. Unlike traditional terrestrial base stations, the agility of ABSs introduces various new approaches to enhance the coverage of wireless networks. ABSs can be utilized as aerial communication platforms to enhance terrestrial communications in the context of 5G, commonly known as ABS-aided terrestrial communications [1]. ABSs can efficiently provide temporary connections to devices that lack coverage. An appealing characteristic of ABSs is their increased likelihood of establishing line-of-sight (LoS) links with ground users, resulting in enhanced received signal quality compared to non-line-of-sight (NLoS) links.

The applications of ABSs span a wide range, encompassing search-and-rescue missions, firefighting, and surveillance. Leveraging these capabilities, ABS networks are commonly structured to transmit control commands and substantial data packages (such as videos) to users [2]. Hence, the majority of ABSs systems necessitate rapid responses and high data rate links. In pursuit of this, the Terahertz (THz) band (0.1–10 THz), with its extensive bandwidth resources, emerges as an ideal choice for the carrier frequency with the potential to deliver unparalleled data rates for the networks of the next generation. Although THz signals may experience considerable path loss, the likelihood of favorable signal propagation from ABS THz base stations to users remains generally high. This is owing to the ABSs' capability to modify their coverage area according to the users they need to serve and the surrounding environment. Consequently, they can effectively minimize path loss. Moreover, THz antennas can be quite compact hence they are suitable for mounting on ABSs [3]. As such, the extensive spectrum available in THz has the potential to significantly enhance the capacity of ABS networks, meeting the need for rapid responses. Furthermore, the data traffic within ABS networks can be substantially increased, given that THz communications excel in providing high throughput for short-range transmissions.

Considerable research has been carried out on evaluating the performance of ABS networks. For instance, in [4], ABSs' positions are modeled as Poisson point processes (PPP). In [5], the ABSs tier is modeled using the binomial point process (BPP) with terrestrial base stations tier following the PPP. The ABSs are modeled using the BPP and are equipped with a cache in [6]. Research on THz ABS networks has been limited. The work in [7] explored a THz ABS network and focused on power allocation and trajectory optimization. In [8], a 2D THz ABS network has been modeled, where the coverage probability (CP) is analyzed. The authors in [9] extend the work in [8] to the 3D model and focus on CP and energy efficiency. Although the aforementioned research work in [8], [9] studies the CP of ABSs-THz network, however, they consider infinite PPP as spatial locations of ABSs. While the PPP has emerged as a canonical model for the spatial distribution of terrestrial base stations, it proves less fitting for ABS networks, particularly evident when a relatively small number of ABSs are deployed to cover a specific finite region [5]. In such situations, realistic modeling of the spatial distribution of ABSs is the BPP while also assuring the tractability of mathematical analysis. Additionally, the BPP captivates for the variableness in performance associated with a particular user location [10].

Motivated by the above considerations, we are interested in developing an analytical framework using stochastic geometry to analyze the coverage performance of a THz ABS wireless network within a finite area. Unlike the work in [8] and [9], we model the location distribution of the ABSs using the BPP model in a finite circular area in a 3D coordinate. To the best of our knowledge, the coverage analysis of THz ABS network in a finite area using BPP model has not been studied previously in the literature. Furthermore, we use the Nakagami-m fading to model the small-scale fading. Under a detailed LoS and NLoS air-to-ground channel model, we derive the coverage probability for the THz ABS network. We consider a probabilistic LoS and NLoS propagation model, cell

associations, and the Laplace transform of interference power in deriving the coverage probability. Our analytical expression is validated through Monte Carlo simulations, confirming its accuracy. The impact of different system parameters on the coverage probability performance has been also investigated.

II. System Model

We consider an ABS wireless network with THz transmission in a 3D coordinate system as shown in Fig.1. The network consists of N ABSs hovering at the same altitude h_A to serve a number of terrestrial users which are randomly distributed on a circular area $\mathbb{R}^2$ with radius r_c. The spatial distribution of the ABSs follows a uniform BPP that forms $\Psi = \{A_i, i = 1 : N\}$, where A_i represents an ABS and its location. To perform our downlink performance analysis, we assume that a reference user U is typically positioned at a distance d_0 from the origin.

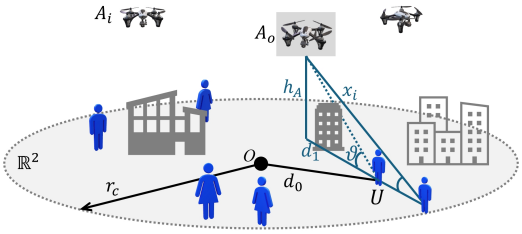

Fig. 1: System model

A. Channel Model

We consider the Air-to-Ground (A2G) channel model for the link between an arbitrary ABS A_o and the reference user U, in which both a LoS link and an NLoS link are considered. The LoS probability P_L between A_o and U is a function of the elevation angle ϑ as in [11], where $\vartheta = \arcsin\left(\frac{h_A}{x}\right)$. For a fixed ABS's height, the LoS probability is a function of x, then the LoS probability can be expressed as $P_L(x) = 1/(1 + ce^{-b(\arcsin(h_A/x)-c)})$, where b and c are environment-dependent parameters, $x = \sqrt{{h_A}^2 + {d_1}^2}$ is the Euclidean distance from A_o to U, and d_1 is the horizontal distance between the projection of A_o and U. Meanwhile, the probability of a NLoS link between A_o and U can be written as $P_N(x) = 1 - P_L(x)$. THz communication is significantly affected by the loss of molecular absorption of water molecules. Consequently, large-scale fading is represented by a deterministic exponential power loss propagation model [12]. We use the Nakagami-m fading to model the small-scale fading with parameters m_L for LoS and m_N NLoS. Thus, the channel fading in LoS and NLoS are h_L and h_N follow Gamma distribution with shape and scale parameters $(m_L, 1/m_L)$ and $(m_N, 1/m_N)$ and the complementary cumulative distribution function (CCDF) can be expressed as $F_{h_\varepsilon}(x) = \sum_{q=0}^{m_\varepsilon - 1} \frac{(m_\varepsilon x)^q}{q!} \exp(-m_\varepsilon x)$, where $\varepsilon \in \{L, N\}$.

We consider a directional antenna model for all the nodes in the system, as described in [13]

$$G(\Theta) = \begin{cases} G_y, & |\Theta| \le b_y \\ g_y, & |\Theta| > b_y \end{cases}, \quad (1)$$

where $y \in \{A, U\}$ denotes either the ABS or the user U, $\Theta \in (-\pi, \pi)$ is the angle of the boresight direction, G_y and g_y are the main lobe and side lobe beamforming gains, and b_y is the main lobe beamwidth. Both U and its associated ABS steer their directional antennas to enhance the gain in directionality. Note that we only consider the main lobe gains between U and its serving ABS A_o. Therefore, the received signal power by U from the LoS and NLoS links can be expressed as $\zeta_L = P_A G_A G_U h_L \mathcal{L} x^{-\alpha_{\mathrm{L}}} e^{-K(f)x}$ and $\zeta_N = P_A G_A G_U h_N \mathcal{L} x^{-\alpha_{\mathrm{N}}} e^{-K(f)x}$, respectively. Where P_A is the transmitter power ABS, G_A and G_U are the main lobe gain of the directional antenna at the ABS and user U respectively, $\mathcal{L} = (\frac{c}{4\pi f})^2$ is the frequency dependent coefficient, where f is the operating frequency and c is the speed of light, α_{L} and α_{N} are the path loss exponents for LoS and NLoS links, respectively, and $K(f)$ is the total molecular absorption coefficient.

When the reference user is associated with one ABS with main lobe gain, the other ABSs may interfere with the associated link. Note that the antennas of these interfering ABSs may not be directly steered toward the reference user, who may experience interference from either the directional antenna's main lobe or the side lobe. Thus, the directionality gain G_{T,x_i} between the U and an interferer is determined as a random variable G_a, $(a \in \{1, 2, 3, 4\})$ which can take values from $\{G_U G_A, G_U g_A, g_U G_A, g_U g_A\}$, and probability p_a for each case is $\{\frac{\Theta_U}{2\pi}\frac{\Theta_A}{2\pi}, \frac{\Theta_U}{2\pi}(1-\frac{\Theta_A}{2\pi}), (1-\frac{\Theta_U}{2\pi})\frac{\Theta_A}{2\pi}, (1-\frac{\Theta_U}{2\pi})(1-\frac{\Theta_A}{2\pi})\}$.

Then the aggregate interference at U from the i-th LoS and NLoS interfering ABSs excluding the serving LoS ABS

$$I_{agg}^{L} = \sum_{i \in \psi_L / A_o} \Lambda x_i^{-\alpha_{\mathrm{L}}} e^{-K(f)x_i} + \sum_{i \in \psi_N} \Lambda x_i^{-\alpha_{\mathrm{N}}} e^{-K(f)x_i}, \quad (2)$$

and the aggregate interference at U from the i-th LoS and NLoS interfering ABSs excluding the serving NLoS ABS

$$I_{agg}^{N} = \sum_{i \in \Psi_L} \Lambda x_i^{-\alpha_{\mathrm{L}}} e^{-K(f)x_i} + \sum_{i \in \Psi_N / A_o} \Lambda x_i^{-\alpha_{\mathrm{N}}} e^{-K(f)x_i}, \quad (3)$$

where $\Lambda = P_A G_{T,x_i} h_\varepsilon$, where $\varepsilon \in \{L, N\}$.

B. User Association Policy

We consider an association strategy that links a user to the ABS offering the highest averaged received signal power [14]. The association options for U are a LoS ABS (LA) or a NLoS ABS (NA) depending on the strongest received signal power. The serving ABS is given as $\arg\max\{P_A G_A G_U h_L \mathcal{L} d_L^{-\alpha_{\mathrm{L}}} e^{-K(f)d_L}, P_A G_A G_U h_N \mathcal{L} d_N^{-\alpha_{\mathrm{N}}} e^{-K(f)d_N}\}$ where $d_L = \min_{\forall x_i \in \Psi_L} d_{L,x_i}$ and $d_N = \min_{\forall x_i \in \Psi_N} d_{N,x_i}$ are the distances of the nearest LA and NA respectively.

III. Association Probabilities and Relevant Distance Distributions

A. Distance Distributions

Given that the ABSs are distributed according to a BPP in a finite area $\mathbb{R}^2$ with a radius of r_c, the probability density function (PDF) for the distance distribution (X_i) between an arbitrary A_o and U is provided according to [15] as:

$$f_{X_i}(x) = \begin{cases} \frac{2x_i}{{r_c}^2}, & h_A \le x_i \le x_m \\ \frac{2x_i}{\pi {r_c}^2} \arccos\left(\frac{{x_i}^2 - {h_A}^2 + {d_0}^2 - {r_c}^2}{2d_0\sqrt{{x_i}^2 - {h_A}^2}}\right), & x_m \le x_i \le x_u, \end{cases} \quad (4)$$

where $x_m = \sqrt{(r_c - d_0)^2 + {h_A}^2}$, and $x_u = \sqrt{(r_c + d_0)^2 + {h_A}^2}$. From the above, we notice that all ABSs are at least at a distance h_A from U. When the reference user U associates with an ABS according to the association policy, for each association, there will be a lower bound of the distance between U and the interference ABSs.

Lemma 1. *When the U associates with the LA located at r with average received power ζ_L, the distance that separates the closest NA from U is denoted as $\mathcal{D}_1(r)$. When the U associates with the NA, the distance that separates the closest LA from U is $\mathcal{D}_2(r)$ and can be obtained as*

$$\mathcal{D}_1(r) = \frac{\alpha_N}{K(f)} \mathcal{W}\left(\frac{K(f)}{\alpha_N}\left(\frac{r^{\alpha_L}}{e^{-K(f)r}}\right)^{\frac{1}{\alpha_N}}\right), \quad (5)$$

$$\mathcal{D}_2(r) = \frac{\alpha_L}{K(f)} \mathcal{W}\left(\frac{K(f)}{\alpha_L} \times \left(\frac{r^{\alpha_N}}{e^{-K(f)r}}\right)^{\frac{1}{\alpha_L}}\right). \quad (6)$$

Proof. The distance $\mathcal{D}_1(r)$ which separates the closest NA from U can be determined by solving the corresponding signal power equations: $P_A G_A G_U \mathcal{L} r^{-\alpha_L} e^{-K(f)r} = P_A G_A G_U \mathcal{L} \mathcal{D}_1(r)^{-\alpha_N} e^{-K(f)\mathcal{D}_1(r)}$. Where $\mathcal{W}[\cdot]$ is the *Lambert W function*. A similar approach can be applied for the distance $\mathcal{D}_2(r)$. □

B. Association Probability

Following the association policy in Section II, in the next Lemma, we will derive the association probabilities.

Lemma 2. *The probabilities that the U being served by either LA or NA are represented by the LoS association probability $\mathcal{A}_{LA}$ and a NLoS association probability $\mathcal{A}_{NA}$ respectively and they are defined as follows*

$$\mathcal{A}_{LA} = N \int_{h_A}^{x_u} P_L(r) f_{Xi}(r) \left(\int_r^{x_u} P_L(x) f_{X_i}(x)\, dx + \int_{\mathcal{D}_1(r)}^{x_u} P_N(x) f_{X_i}(x)\, dx\right)^{N-1} dr, \quad (7)$$

$$\mathcal{A}_{NA} = N \int_{h_A}^{x_u} P_N(r) f_{Xi}(r) \left(\int_r^{x_u} P_N(x) f_{X_i}(x)\, dx + \int_{\mathcal{D}_2(r)}^{x_u} P_L(x) f_{X_i}(x)\, dx\right)^{N-1} dr. \quad (8)$$

Proof. To derive $\mathcal{A}_{LA}$, we first consider an arbitrary ABS located at a distance r from U. The $\mathcal{A}_{LA}$ association happens when two events are simultaneously achieved. The first event occurs when the ABS has a LoS link with LoS probability $P_L(r)$. The second event occurs when the average signal power received from this ABS is larger than that received from the remaining ABSs. Thus, the remaining ABSs are either a LoS ABS further than r, or a NLoS ABS located beyond $\mathcal{D}_1(r)$. The probabilities of those are $\int_r^{x_u} P_L(x) f_{X_i}(x)\, dx$ and $\int_{\mathcal{D}_1(r)}^{x_u} P_N(x) f_{X_i}(x)\, dx$. As the two probabilities are mutually exclusive and the remaining ABSs $(N-1)$ are i.i.d, then the probability of the second event is $\left(\int_r^{x_u} P_L(x) f_{X_i}(x)\, dx + \int_{\mathcal{D}_1(r)}^{x_u} P_N(x) f_{X_i}(x)\, dx\right)^{N-1}$. Thus, the probability of LA being the serving ABS can be obtained by multiplying the above probabilities as they are independent $P_L(r)\left(\int_r^{x_u} P_L(x) f_{X_i}(x)\, dx + \int_{\mathcal{D}_1(r)}^{x_u} P_N(x) f_{X_i}(x)\, dx\right)^{N-1}$. Then $\mathcal{A}_{LA}$ can be derived by integrating over $h_A \le r \le x_u$ as in (7). The derivation of the association $\mathcal{A}_{NA}$ in (8) follows the same approach as LA thus omitted. □

C. Serving and Interference Distance Distributions

1) Conditional Serving Distance Distribution: To derive the coverage probability, we need to derive the serving distance distribution and the interference distance distribution for each association condition. The cumulative distribution function (CDF) of the serving distance R_L between a LoS ABS and the U is denoted by $F(R_L)$

$$F_{R_L}(r) = \frac{P(R_L < r)}{P(LA)} = \frac{N}{\mathcal{A}_{LA}} \int_{h_A}^{r} P_L(z) f_{Xi}(z) \left[\int_r^{x_u} P_L(x) f_{X_i}(x)\, dx + \int_{\mathcal{D}_1(r)}^{x_u} P_N(x) f_{X_i}(x)\, dx\right]^{N-1} dz, \quad (9)$$

where $P(LA)$ is equal to $\mathcal{A}_{LA}$. Thus, the PDF of $F(R_L)$ can be obtained by taking the derivative

$$f_{R_L}(r) = \frac{dF_{R_L}(r)}{dr} = \frac{N P_L(r) f_{Xi}(r)}{\mathcal{A}_{LA}} \left(\int_r^{x_u} P_L(x) f_{X_i}(x)\, dx + \int_{\mathcal{D}_1(r)}^{x_u} P_N(x) f_{X_i}(x)\, dx\right)^{N-1}. \quad (10)$$

The PDF of the serving distance R_N between a NLoS ABS and the U can be obtained following a similar approach

$$f_{R_N}(r) = \frac{N P_N(r) f_{Xi}(r)}{\mathcal{A}_{NA}} \left(\int_r^{x_u} P_N(x) f_{X_i}(x)\, dx + \int_{\mathcal{D}_2(r)}^{x_u} P_L(x) f_{X_i}(x)\, dx\right)^{N-1}. \quad (11)$$

2) Conditional Interference Distance Distribution: The reference user may be interfered by other ABSs. Let R_Q be the serving distance between the U and the serving ABS either LA or NA, $Q \in \{LA, NA\}$. Then the interference distance between U and an interfering ABS A_i is denoted as $W_{i|QLA}/W_{i|QNA}$ under the condition that $R_Q = r$ and the A_o is a LA or NA. Then the PDF of $W_{i|QY}$ is obtained as in [5, Lemma 4], $f_{W_{i|QY}}(w|R_Q = r) = \frac{P_Y(w) f_{X_i}(w)}{\int_{\mathcal{D}_{QY}(r)}^{x_u} P_Y(x) f_{X_i}(x)\, dx}$, where Y is an interfering ABS and $Y \in \{LA, NA\}$.

IV. Coverage Probability

We aim to analyze the coverage probability in the downlink of the THz ABS system. The coverage probability P_C is defined as the probability that the signal-to-noise-plus-interference ratio (SINR) γ at the user exceeds a predetermined threshold T, i.e. $P_C = P(\gamma \ge T)$. When U is associated with LA, the SINR can be expressed as $\gamma_L = \frac{\zeta_L}{I_{agg}^L + N_0}$. When U is associated with a NA, the SINR can be expressed as $\gamma_N = \frac{\zeta_N}{I_{agg}^N + N_0}$, where N_0 represents the thermal noise power. Since U can be associated with either LA or NA, P_C can be obtained by $P_C = \mathcal{A}_{LA} P_{C,L} + \mathcal{A}_{NA} P_{C,N}$. Where $\mathcal{A}_{LA}$ and $\mathcal{A}_{NA}$ are the association probabilities, and $P_{C,L}$ and $P_{C,N}$ are the corresponding conditional coverage probabilities.

Theorem 1. *The conditional coverage probabilities that the U is served by LA or NA are denoted as $P_{C,L}$ and $P_{C,N}$, and are given as below*

$$P_{C,\varepsilon} = \int_{h_a}^{x_u} \sum_{q=0}^{m_{\mathrm{L}}-1} \frac{(-s_L)^q}{q!} \sum_{u=0}^{q} \binom{q}{u} (-N_0)^{(q-u)} \exp\left(-s_\varepsilon N_0\right) \frac{\partial^u}{\partial s_\varepsilon^u} L_{I_{agg}^{\varepsilon}}(s_\varepsilon)\, f_{R_\varepsilon}(r)\, dr, \tag{12}$$

where $\varepsilon \in \{L, N\}$, $s_\varepsilon = \frac{m_\varepsilon T}{P_A G_A G_U \varepsilon r^{-\alpha_\varepsilon} e^{-K(f)r}}$, $L_{I_{agg}^{\varepsilon}}(.)$ is the Laplace transform (LT) of the aggregate interference.

Proof.

$$P_{C,L} = P(\gamma_L \geq T|LA) = P\left(\frac{\zeta_L}{I_{agg}^L + N_0} \geq T|LA\right)$$

$$= \int_{h_a}^{x_u} f_{R_L}(r) \underbrace{P\left(\frac{\zeta_L}{I_{agg}^L + N_0} \geq T|LA, r\right)}_{\Delta(r)} dr,$$

$$\Delta(r) = P\left(\frac{P_A G_A G_U h_L \mathcal{L} r^{-\alpha_{\mathrm{L}}} e^{-K(f)r}}{I_{agg}^L + N_0} \geq T|LA, r\right)$$

$$\overset{(a)}{=} \mathbb{E}_{[r, I_{agg}^L]}\left[P\left(h_L \geq \frac{T(I_{agg}^L + N_0)}{P_A G_A G_U \mathcal{L} r^{-\alpha_{\mathrm{L}}} e^{-K(f)r}}\right)\right]$$

$$\overset{(b)}{=} \mathbb{E}_{x_{\mathrm{L}}, I_{\mathrm{L}}}\left[\sum_{q=0}^{m_{\mathrm{L}}-1} \frac{1}{q!}\left(\frac{m_{\mathrm{L}} T(I_{agg}^L + N_0)}{P_A G_A G_U \mathcal{L} r^{-\alpha_{\mathrm{L}}} e^{-K(f)r}}\right)^q \times \exp\left(-\frac{T(I_{agg}^L + N_0)}{P_A G_A G_U \mathcal{L} r^{-\alpha_{\mathrm{L}}} e^{-K(f)r}}\right)\right]$$

$$\overset{(c)}{=} \mathbb{E}_{x_{\mathrm{L}}, I_{\mathrm{L}}}\left[\sum_{q=0}^{m_{\mathrm{L}}-1} \frac{(s_L)^q}{q!}\left(I_{agg}^L + N_0\right)^q \exp\left(-s_L(I_{agg}^L + N_0)\right)\right]$$

$$\overset{(d)}{=} \sum_{q=0}^{m_{\mathrm{L}}-1} \frac{(-s_L)^q}{q!}\left[\frac{\partial^q}{\partial s_L^q} \exp\left(-s_L N_0\right) \times L_{I_{agg}^L}(s_L)\right], \tag{13}$$

where (a) follows averaging over the independent random variables r and I_{agg}^L, (b) according to the CCDF of h_L, (c) from $s_L = \frac{m_L T}{P_A G_A G_U \mathcal{L} r^{-\alpha_{\mathrm{L}}} e^{-K(f)r}}$, (d) from the LT definition of the interference $\mathbb{E}_{[I_{agg}^L]}\left[\exp\left(-s_L I_{agg}^L\right)\right]$. The final expression in (12) is obtained by applying the expression $\frac{\partial^q}{\partial x^q} f(x)g(x) = \sum_{u=0}^{q} \binom{q}{u} \frac{\partial^u}{\partial x^u} f(x) \frac{\partial^{q-u}}{\partial x^{q-u}} g(x)$. The conditional converge probability $P_{C,N}$ can be derived following a similar approach, thus the detailed proof is omitted here. □

Lemma 3. *The LT of the interference from A_i when U is associated with LA at a distance R_L, and when U is associated with NA at a distance R_N can given by*

$$L_{I_{agg}^L}(s_L) = \Bigg[P_{L|LA}^i \sum_{a=1}^{4} p_a \int_{R_L}^{x_u} f_{W_{i|LL}}(w|R_L = r) \times \left(1 + \frac{s_L P_A G_a \mathcal{L} w^{-\alpha_{\mathrm{L}}} e^{-K(f)w}}{m_L}\right)^{-m_L} dw,$$

$$+ P_{N|LA}^i \sum_{a=1}^{4} p_a \int_{\mathcal{D}_1(R_L)}^{x_u} f_{W_{i|LN}}(w|R_L = r) \times \left(1 + \frac{s_L P_A G_a \mathcal{L} w^{-\alpha_{\mathrm{N}}} e^{-K(f)w}}{m_N}\right)^{-m_N} dw\Bigg]^{N-1}, \tag{14}$$

$$L_{I_{agg}^N}(s_N) = \Bigg[P_{L|NA}^i \sum_{a=1}^{4} p_a \int_{\mathcal{D}_2(R_N)}^{x_u} f_{W_{i|NL}}(w|R_N = r) \times \left(1 + \frac{s_N P_A G_a \mathcal{L} w^{-\alpha_{\mathrm{L}}} e^{-K(f)w}}{m_L}\right)^{-m_L} dw$$

$$+ P_{N|NA}^i \sum_{a=1}^{4} p_a \int_{R_N}^{x_u} f_{W_{i|NN}}(w|R_N = r) \times \left(1 + \frac{s_N P_A G_a \mathcal{L} w^{-\alpha_{\mathrm{N}}} e^{-K(f)w}}{m_N}\right)^{-m_N} dw\Bigg]^{N-1}. \tag{15}$$

Proof. Let $L_{I_{\mathrm{agg}}^L}(s_L)$ be the LT of the interference from A_i where U is associated with LA at a distance R_L. Then the interference can be either a LA located at a distance greater than R_L or an NA located at a distance greater than $\mathcal{D}_1(R_L)$. The probabilities of these events are denoted as $P_{L|LA}^i$ and $P_{N|LA}^i$ can be expressed as

$$P_{L|LA}^i = \frac{\int_{R_L}^{x_u} P_L(x) f_{X_i}(x)\, dx}{\left(\int_{R_L}^{x_u} P_L(x) f_{X_i}(x)\, dx + \int_{\mathcal{D}_1(R_L)}^{x_u} P_N(x) f_{X_i}(x)\, dx\right)}, \tag{16}$$

$$P_{N|LA}^i = \frac{\int_{\mathcal{D}_1(R_L)}^{x_u} P_N(x) f_{X_i}(x)\, dx}{\left(\int_{R_L}^{x_u} P_L(x) f_{X_i}(x)\, dx + \int_{\mathcal{D}_1(R_L)}^{x_u} P_N(x) f_{X_i}(x)\, dx\right)}, \tag{17}$$

then
$$L_{I_{\mathrm{agg}}^L}(s_L) = P_{L|LA}^i \mathbb{E}_{[P_{I_L}]}(\exp\left(-s_L P_{I_L}\right)) + P_{N|LA}^i \mathbb{E}_{[P_{I_N}]}(\exp\left(-s_L P_{I_N}\right)), \tag{18}$$

where P_{I_L} and P_{I_N} are the received power from the interfering LA and NA given in section II. After averaging over G_T and the small scale fading

$$\mathbb{E}_{[P_{I_L}]}(\exp\left(-s_L P_{I_L}\right)) = \sum_{a=1}^{4} p_a \int_{R_L}^{x_u} f_{W_{i|LL}}(w|R_L = r) \left(1 + \frac{s_L P_A G_a \mathcal{L} w^{-\alpha_{\mathrm{L}}} e^{-K(f)w}}{m_L}\right)^{-m_L} dw, \tag{19}$$

$$\mathbb{E}_{[P_{I_N}]}(\exp\left(-s_L P_{I_N}\right)) = \sum_{a=1}^{4} p_a \int_{\mathcal{D}_1(R_L)}^{x_u} f_{W_{i|LN}}(w|R_L = r) \left(1 + \frac{s_L P_A G_a \mathcal{L} w^{-\alpha_{\mathrm{N}}} e^{-K(f)w}}{m_N}\right)^{-m_N} dw, \tag{20}$$

then the expression $L_{I_{\mathrm{agg}}^L}(s_L)$ in (14) can be obtained by plugging in (19) and (20) in (18). A similar approach can be followed to derive the LT of the interference $L_{I_{\mathrm{agg}}^N}(s_N)$. □

V. Numerical Results and Discussion

In this section, we evaluate the performance of the system by presenting numerical results. We first validate the analytical coverage probability using Monte Carlo simulation with 10^5 iterations, then we examine the impact of different system parameters on the coverage performance. Assuming a dense urban environment, the environmental parameters $b = 0.136$ and $c = 11.95$ [5], $\alpha_{\mathrm{L}} = 2$, $\alpha_{\mathrm{N}} = 4$, P_A = 10 dBm, G_A = 25 dBi, g_A = -10 dBi, G_U = 10 dBi, g_U = -10 dBi, $\Theta_A = 10°$, $\Theta_U = 33°$, $N_o = 4 \times 10^{-11}$ Watt, f = 1 THz, $K(f)$ = 0.07512 m^{-1}, m_L=3 and m_N=1.

In Fig. 2, we compare the analytical coverage probability with Monte Carlo simulation results under different ABS

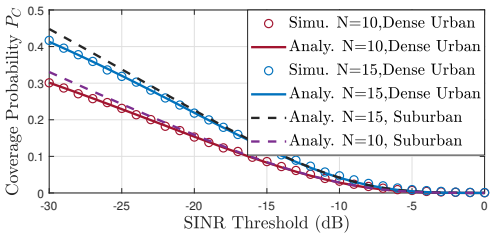

Fig. 2: P_C vs T, $h_A = 80$m, $r_c = 500$m, $d_1 = 0$m, Suburban ($b = 0.1581$ and $c = 9.6117$).

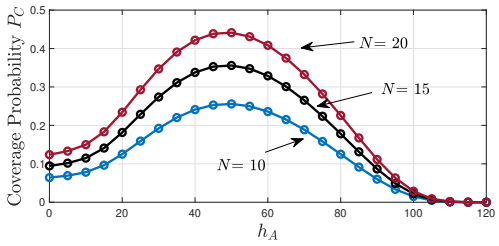

Fig. 3: P_C vs h_A, $r_c = 400$ m, T = -15 dB and $d_1 = 0$ m.

numbers N. The analytical results are demonstrated to match the simulation results and the coverage probability decreases as the SINR threshold increases. In addition, the coverage probability improves as the number of ABS N increases. Furthermore, the coverage is higher in suburban environment due to fewer obstacles and improved LoS as shown in the dashed curves. In Fig. 3, we illustrate the impact of the ABS altitude h_A on the coverage probability across different ABS numbers N. We can observe that at lower ABS altitudes, the coverage probability is minimal but escalates swiftly as the altitude increases. This phenomenon stems from the elevation angle between the U and the ABS, which rises with increasing ABS altitude, thereby enhancing the likelihood of establishing a LoS connection. However, it is also revealed in the figure that there exists an optimal ABS altitude for maximizing coverage probability. Beyond this threshold, further altitude increments do not yield additional benefits in coverage probability. This is attributed to the fact that transmissions beyond this optimal altitude predominantly form LoS links, and any extension in transmission distance adversely affects signal quality. Fig. 4 shows the impact of the radius r_c on the coverage probability. The depicted trend reveals that as the radius expands, the coverage probability will monotonically decrease. While deploying ABSs at higher altitudes mitigates the degradation in coverage probability to some extent, the loss in performance remains irreversible as the radius expands.

VI. Conclusion

In this paper, we have analyzed the coverage performance of a THz ABS network. The spatial location of the ABSs is modeled as a BPP model in a finite circular area. Based on tools from stochastic geometry, we derived the coverage probability with a consideration of the probabilistic LoS and NLoS propagation models, cell associations, and the Laplace transform of interference power distribution after characterizing the distance distributions. We validated the precision of the derived analytical expression via Monte Carlo simulation and examined how key system parameters influence the coverage probability performance. Simulation results show that the height of the ABS, the radius of the area, and the

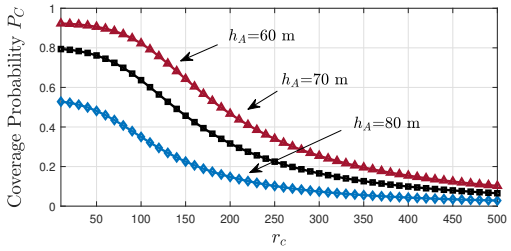

Fig. 4: P_C vs r_c , $T = -10$dB and $d_1 = 0$ m.

number of ABSs should be carefully selected to achieve better performance. The THz-specific path loss model results in a more decrease in signal strength with distance, necessitating a denser ABS network for effective coverage. Additionally, it identifies a different optimal altitude for ABS deployment compared to non-THz networks.

Acknowledgment

This work was supported by the Finnish Cultural Foundation and the Information Technology Research Foundation, Finland, and partially supported by the DIOR project (10100828) which has received funding from the European Union's MSCA RISE programme.

References

[1] N. Zhao, W. Lu, M. Sheng, Y. Chen, J. Tang, F. R. Yu, and K.-K. Wong, "Uav-assisted emergency networks in disasters," *IEEE Wireless Communications*, vol. 26, no. 1, pp. 45–51, 2019.

[2] Z. Xiao, P. Xia, and X.-g. Xia, "Enabling uav cellular with millimeter-wave communication: potentials and approaches," *IEEE Communications Magazine*, vol. 54, no. 5, pp. 66–73, 2016.

[3] H. Elayan, O. Amin, R. M. Shubair, and M.-S. Alouini, "Terahertz communication: The opportunities of wireless technology beyond 5g," in *2018 International Conference on Advanced Communication Technologies and Networking (CommNet)*, 2018, pp. 1–5.

[4] J. Peng, W. Tang, and H. Zhang, "Directional antennas modeling and coverage analysis of uav-assisted networks," *IEEE Wireless Commun. Lett.*, vol. 11, no. 10, pp. 2175–2179, 2022.

[5] X. Wang, H. Zhang, Y. Tian, and V. C. M. Leung, "Modeling and analysis of aerial base station-assisted cellular networks in finite areas under los and nlos propagation," *IEEE Trans. Wireless Commun.*, vol. 17, no. 10, pp. 6985–7000, 2018.

[6] Q. Zhu, J. Zheng, and A. Jamalipour, "Coverage performance analysis of a cache-enabled uav base station assisted cellular network," *IEEE Trans. Wireless Commun.*, vol. 22, no. 11, pp. 8454–8467, 2023.

[7] S. Farrag, E. Maher, A. El-Mahdy, and F. Dressler, "Performance analysis of uav assisted mobile communications in thz channel," *IEEE Access*, vol. 9, pp. 160 104–160 115, 2021.

[8] X. Wang, P. Wang, M. Ding, Z. Lin, F. Lin, B. Vucetic, and L. Hanzo, "Performance analysis of terahertz unmanned aerial vehicular networks," *IEEE Trans. Veh. Technol.*, vol. 69, no. 12, pp. 16 330–16 335, 2020.

[9] K. M. S. Huq, I. E. Otung, and J. Rodriguez, "A study of coverage probability-based energy-efficiency analysis for uav-aided thz-enabled 6g networks," *IEEE Trans. Intell. Transp. Syst.*, vol. 24, no. 7, pp. 7404–7411, 2023.

[10] N. Kouzayha, M. A. Kishk, H. Sarieddeen, M.-S. Alouini, and T. Y. Al-Naffouri, "Coexisting terahertz and rf finite wireless networks: Coverage and rate analysis," *IEEE Trans. Wireless Commun.*, 2022.

[11] A. Al-Hourani, S. Kandeepan, and S. Lardner, "Optimal lap altitude for maximum coverage," *IEEE Wireless Commun. Lett.*, vol. 3, no. 6, pp. 569–572, 2014.

[12] H. Obaid, Y. Zhu, and B. Tan, "Collaborative caching and reconfigurable intelligent surface for the sub-thz mobile system," *IEEE Wireless Commun. Lett.*, pp. 1–1, 2024.

[13] T. Bai and R. W. Heath, "Coverage and rate analysis for millimeter-wave cellular networks," *IEEE Trans. Wireless Commun.*, vol. 14, no. 2, pp. 1100–1114, 2015.

[14] H. Ghazzai, E. Yaacoub, M.-S. Alouini, Z. Dawy, and A. Abu-Dayya, "Optimized lte cell planning with varying spatial and temporal user densities," *IEEE Trans. Veh. Technol.*, no. 3, pp. 1575–1589, 2016.

[15] V. V. Chetlur and H. S. Dhillon, "Downlink coverage analysis for a finite 3-d wireless network of unmanned aerial vehicles," *IEEE Trans. Commun.*, vol. 65, no. 10, pp. 4543–4558, 2017.